International Journal of Microwave and Wireless Technologies

cambridge.org/mrf

Wideband dual-polarized Vivaldi antenna with improved balun feed

Lizhong Song and Huiyuan Zhou

School of Information and Electrical Engineering, Harbin Institute of Technology at Weihai, 264209, P.R. China

Research Paper

Cite this article: Song L, Zhou H (2019). Wideband dual-polarized Vivaldi antenna with improved balun feed. *International Journal of Microwave and Wireless Technologies* **11**, 41–52. https://doi.org/10.1017/S1759078718001113

Received: 26 February 2018
Revised: 28 June 2018
Accepted: 29 June 2018
First published online: 1 August 2018

Key words:
Balun; dual-polarized antenna; radiation pattern; Vivaldi antenna

Author for correspondence:
L. Song, H. Zhou, E-mail: songlz@hit.edu.cn, easy_zhou_easy@163.com

Abstract

The paper researches a kind of wideband dual-polarized Vivaldi antenna with improved balun feed which consists of slot line and two bent coplanar strip lines. The whole of antenna structure is composed of two orthogonal Vivaldi antenna elements, and the mode of feeding adopts electromagnetic coupling from micro-strip line to slot line. The improved balun can avoid the intersection of transmission lines, reduce the size, and simplify the assembly. The electromagnetic simulation and optimization design of proposed antenna are carried out by using electromagnetic simulation software, CST. Simulation results show that the isolation between two polarized ports is more than 15 dB within working frequency range of 2–3.5 GHz and VSWRs of two ports are lower than 2.5 at the range of 2–3.5 GHz. The designed antenna is fabricated and measured. The measured results indicate that the designed antenna achieves anticipated patterns and feasible design of the dual-polarized Vivaldi antenna. The dual-polarized Vivaldi antenna with improved balun feed is suitable for some application fields, such as passive electronic reconnaissance, passive radar, and wideband communication and detection.

Introduction

The electromagnetic waves carry information including amplitude, phase, direction, frequency, and polarization information. Using polarization information on processing technology to develop polarized radar is an effective approach, which solves four intimidations of military radar facing and improves the capability of radar detection and anti-jamming. Dual-polarized antenna can form a pair of work mode with orthogonal polarization and equal frequency at the same time, and then it can receive all of the polarization information, have a strong capability of anti-jamming, improve system sensitivity and work in some application fields such as passive electronic reconnaissance, passive radar, and wideband communication and detection. The design and realization of dual-polarized antennas have become the focus of research in the field of the antenna. Nowadays, the commonly used dual-polarized antenna elements are dual-polarized dipole antennas, dual-polarized micro-strip patch antennas, dual-polarized waveguide slot antennas, and so on. In the design of dual-polarized antenna element, beam width and the isolation between two polarization ports should be considered, besides working frequency range, bandwidth, return loss, gain, and so on. For example, Yang *et al.* researched a wideband ±45° dual-polarized directional antenna with high gains. The isolation between two polarization ports was better than 32 dB and gains were higher than 9.2 dBi at the range of 2.5–3.8 GHz [1]. Yu *et al.* researched a new type of antenna element for wideband wide-angle dual-polarized phased array antennas which was composed of Vivaldi antenna, and achieved electrical connection by using metallic posts [2]. Ren *et al.* presented a wideband and high-gain dual-polarized antenna based on split-ring resonators. The purpose of using metamaterials was to improve antenna gain and broaden the bandwidth [3]. Wang *et al.* presented an antenna merging inverted-cone monopole and cross bow-tie dipole to achieve dual polarizations while maintaining a wide bandwidth [4]. Zhu *et al.* researched a novel dual-polarized patch antenna for ultra-wideband applications which was composed of a square patch and four capacitively coupled feeds to enhance the impedance bandwidth, and the antenna has achieved an impedance bandwidth of 112% [5]. In the literature [6], the advantages of proposed antenna, which adopted Vivaldi antenna element, were ultra-wideband, low cross-polarization, and small dimensions within working frequency range of 3.1–10.6 GHz. In the literature [7], a dual-band dual-polarized end-fire antenna was proposed, that its ISR structure was loaded to improve the gain in end-fire direction. In the literature [8], a simple compact dual-polarized ultra-wideband MIMO antenna was presented with the circularly polarized band for WiMAX (5.5 GHz) and WLAN (5, 5.2 GHz) applications which adopted feed points of micro-strip slot coupling. In conclusion, the common dual-polarized antenna structures are symmetric and asymmetric structures by using basic antenna. The symmetric structures with two antenna elements implementing dual-polarized antenna are same and orthogonally placed. The asymmetric structures are that the two antenna elements to implement dual-

CAMBRIDGE UNIVERSITY PRESS

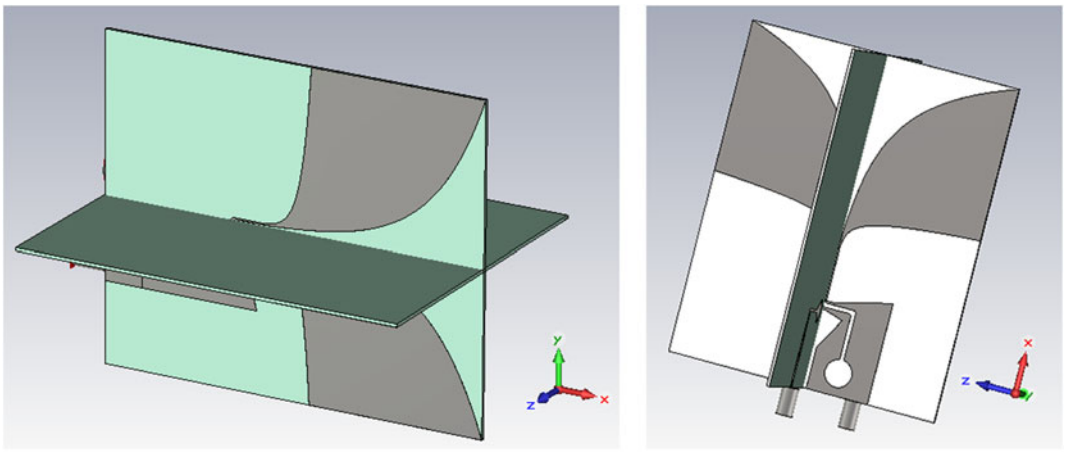

Fig. 1. The perspective of the proposed antenna model.

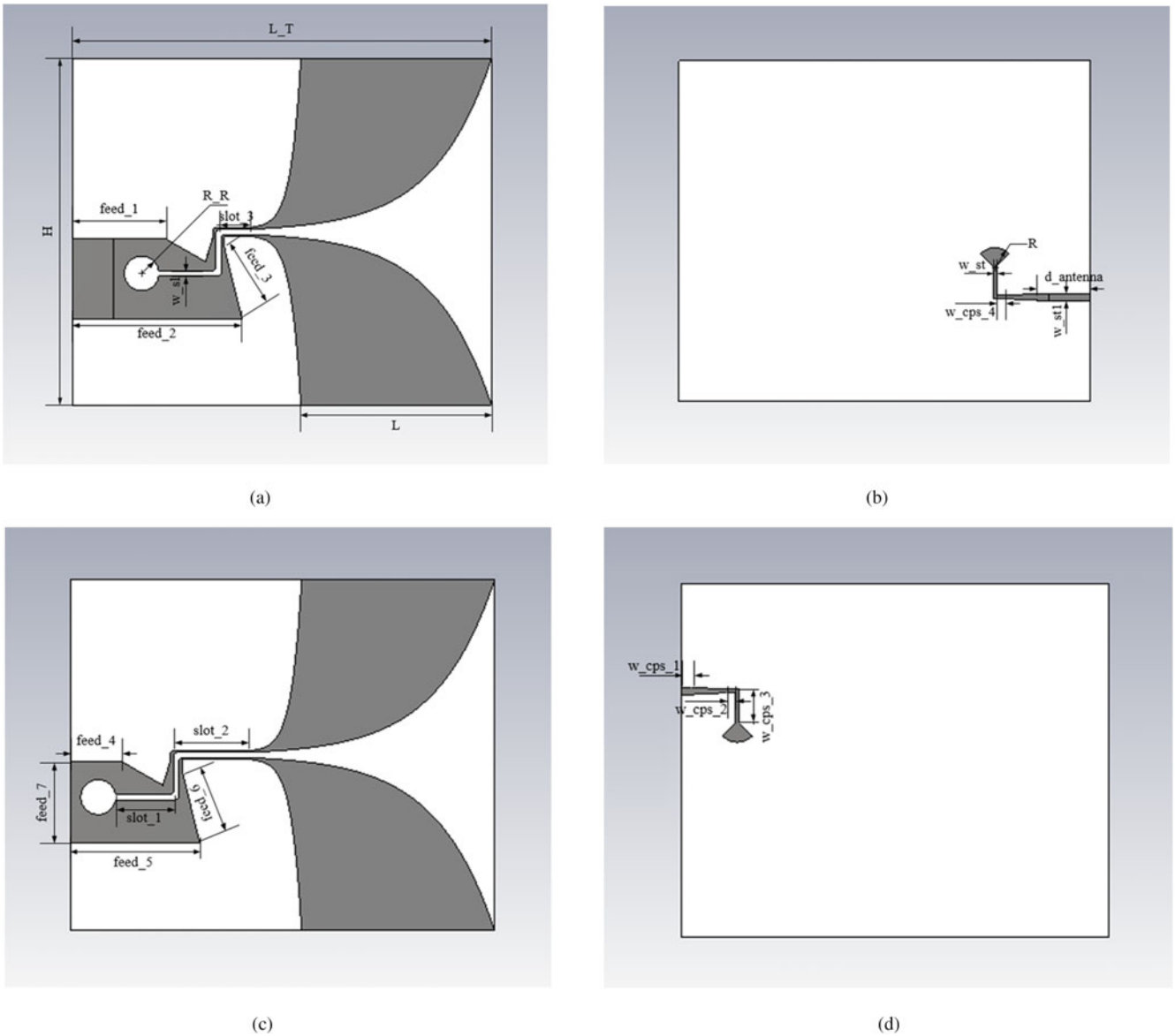

Fig. 2. The engineering drawing of wideband dual-polarized Vivaldi antenna with improved balun, (a) Vivaldi side of engineering drawing of port 1, (b) the feed side of engineering drawing of port 1, (c) Vivaldi side of engineering drawing of port 2, (d) the feed side of engineering drawing of port 2.

https://doi.org/10.1017/S1759078718001113 Published online by Cambridge University Press

Table 1. Parameter table of the presented antenna structure (units: mm)

Parameter	Size	Parameter	Size	Parameter	Size	Parameter	Size	Parameter	Size
L_T	120.94	feed_3	21.32	w_sl	1.5	w_cps	2.5	slot_1	17
H	100	w_st	1	slot_3	9.38	w_st1	2	slot_2	21.38
L	55	feed_7	23	R_R	5	feed_4	14.92	w_cps_l	3
feed_l	26.92	w_cps_4	2.5	R	6	feed_5	36.94	w_cps_2	2.5
feed_2	48.94	w_cps_3	9.5	d_antenna	15	feed_6	21.32		

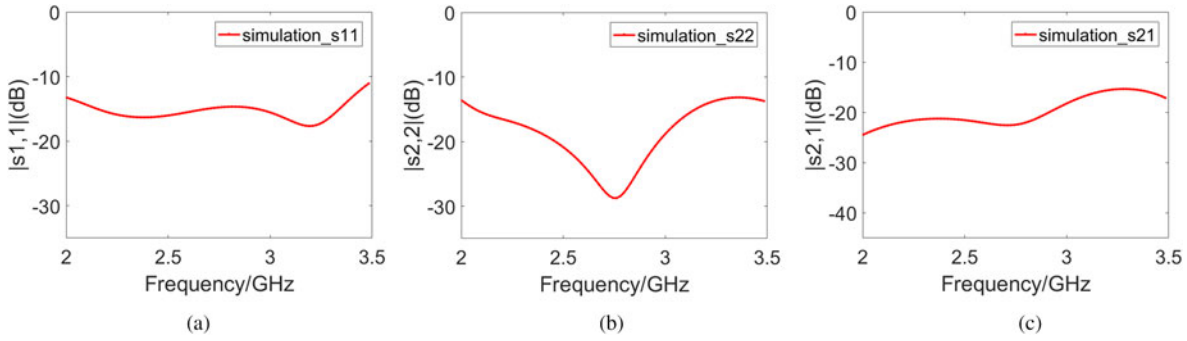

Fig. 3. The simulation results of circuit characteristics, (a) the return loss of port 1, (b) the return loss of port 2, (c) the isolation between two polarization ports.

polarized antenna are different, but this way can implement dual polarization. At the same time, the antenna performance can be improved by adding metamaterials in the antenna, using metamaterials structures and so on.

The feature of Vivaldi antenna includes wideband, low cross-polarization, wide wave beam, and end fire. Its main performance is determined by a slot line which is graded according to the exponential curve. Different open widths radiate different electromagnetic signals. Thus, the maximal opening width of the radiation patch is determined by the minimum operating frequency of the Vivaldi antenna, i.e. the maximal slot size of the radiation patch is $\lambda/2$ (λ is the wavelength value of the lowest working frequency), and the minimal opening width of the radiation patch is determined by the maximum operating frequency. According to the radiation mechanism of Vivaldi antenna, work mechanism is similar to the TEM mode horn antenna. In other words, the *E*-plane metal of the horn antenna is equivalent to the cover on the substrate directly, and the waveguide part of the horn antenna is equivalent to the coupling slot line. The energy is transmitted to the matching cavity by electromagnetic coupling, then passes through the coupling slot line to the open slot line, then along the open slot line direction, and finally is radiated at the corresponding resonant slot line according to a different frequency. Vivaldi antenna is a kind of common antenna in wideband antenna field. The research focuses on the following directions: wideband, multi-band frequency, circular polarization, mode of feeding, and dual polarization. For example, in the literature [9], a wideband, dual-polarized Vivaldi antenna or tapered slot antenna with over a decade of bandwidth was presented which was composed of inserting two orthogonal Vivaldi antennas in a cross-shaped form without a galvanic contact. In the literature [10], an ultra-wideband 2–18 GHz dual-polarized Vivaldi antenna array was presented where the whole of slot line is curved, but this antenna structure was not easy to assemble and an SMP connector was used instead of a typical SMA connector. In the literature [11], an optimized-taper antipodal Vivaldi slot with a bandwidth of 2.5:1 was the dual-polarized antenna element which adopted exponential tapered balun within the operating frequency range of 0.8~4 GHz. In the literature [12], a miniaturized ultra-wideband double-layered Vivaldi antenna was proposed, in which optimized slots are inserted in the radiation patches to obtain a low-frequency resonance at the range of 2.5–11 GHz. Wu *et al.* researched a new wideband circularly polarized antenna array with high gain and low side lobe working in the total X-band; that element was Vivaldi antenna and the method of matching slot line to coaxial line was using Chebyshev impedance convertor [13]. Xu *et al.* presented a novel cross circular-polarized antenna array in which the element was Vivaldi antenna and the edge of the element adopted a saw-tooth structure [14]. Kang *et al.* researched a dual-polarized orthogonal Vivaldi antenna with high port isolation in which its structure was a novel exponentially tapered slot-edge structure [15]. Zhang *et al.* researched an ultra-wideband dual-polarized Vivaldi antenna with low cross-polarization and a choke-slot was added to suppress the surface wave of the antenna to reduce the rear flap of the antenna [16]. To sum up, there are three main features as follow: firstly, many Vivaldi antenna elements commonly adopt slot structure or printed dipole structure; secondly, slot line structure is usually linear; finally, antenna structure is simple and easy to assemble. The antenna structure using curved slot line from the literature [10] was not easy to assemble. One of the technical difficulties of Vivaldi antenna is the design of balun and feed structure. In this paper, a dual-polarized Vivaldi antenna is presented, which is easy to assemble and has an improved new balun. The improved balun consists of two bent coplanar strip lines and a slot line. The improved balun structure avoids the intersection of transmission lines and reduces size.

In this paper, a wideband dual-polarized Vivaldi antenna with improved balun feed is presented, which is suitable to use in some fields. Then the structure of dual-polarized Vivaldi antenna

https://doi.org/10.1017/S1759078718001113 Published online by Cambridge University Press

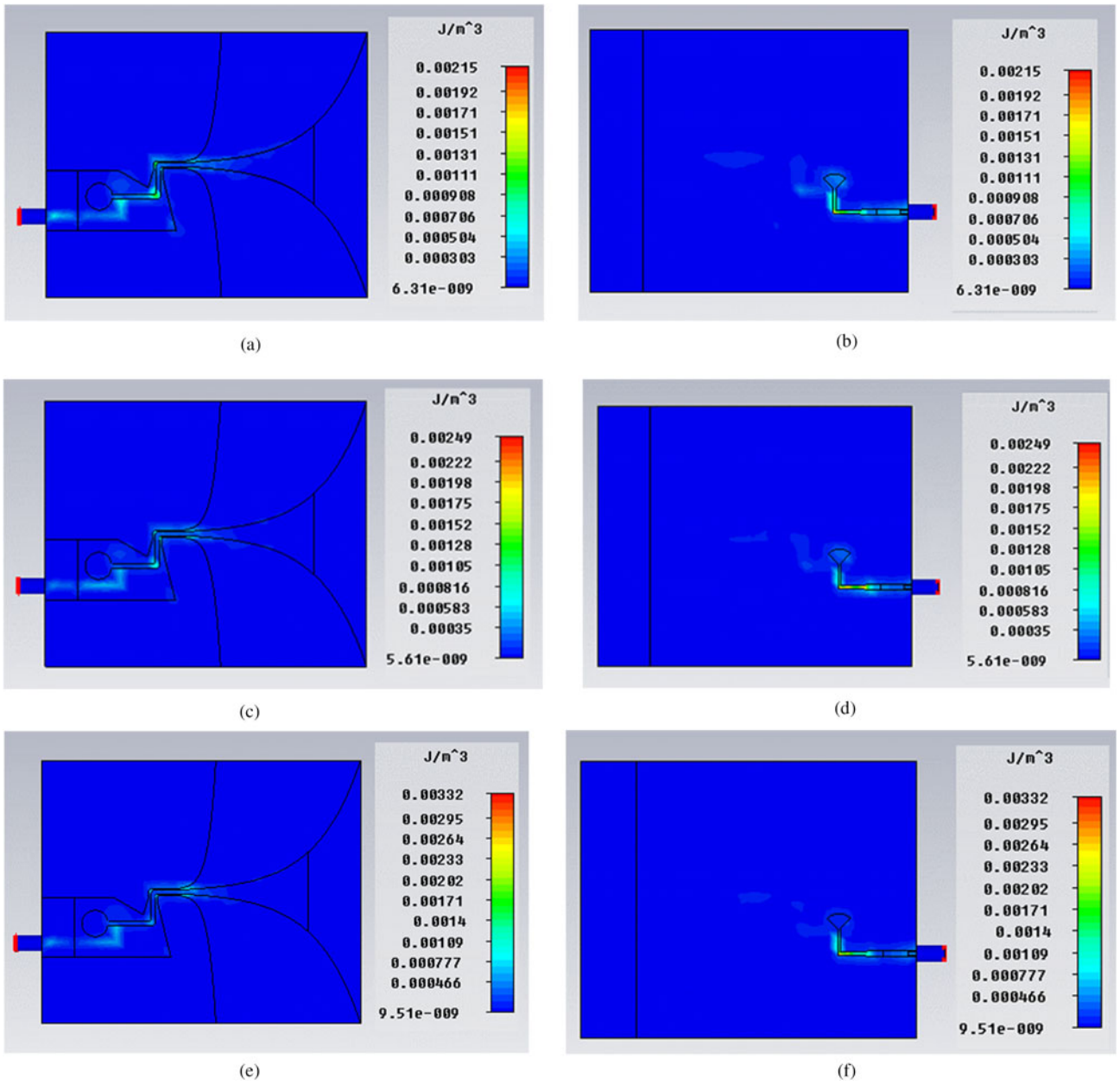

Fig. 4. Simulated electric energy density of port 1, (a) positive structure of electric energy density at 2 GHz, (b) reverse structure of electric energy density at 2 GHz, (c) positive structure of electric energy density at 2.5 GHz, (d) reverse structure of electric energy density at 2.5 GHz, (e) positive structure of electric energy density at 2.7 GHz, (f) reverse structure of electric energy density at 2.7 GHz.

element is designed and simulated through electromagnetic simulation software, CST. After that, the designed dual-polarized Vivaldi antenna is fabricated and measured, and the measured results of impedance characteristics and radiation patterns are provided. Finally, a research conclusion is drawn.

Structure design of the dual-polarized Vivaldi antenna with improved balun feed

In this paper, the structure model of wideband dual-polarized Vivaldi antenna with improved balun feed is presented in Fig. 1. The designed antenna is composed of two Vivaldi antenna elements, which are orthogonally located. The employed dielectric substrate is FR-4 ($\varepsilon_r = 4.3$), for which the substrate thickness is 1 mm and the metal copper foil thickness is 0.036 mm. In order to achieve dual-polarized operating model, each element is fed by employing the electromagnetic coupling from micro-strip line to slot line. The micro-strip line is located on the other side of the dielectric substrate, and a sector-shaped branch structure at the end of the micro-strip line is adopted to achieve impedance matching. The output part of the micro-strip line is connected to the inner conductor of a coaxial cable. The outer conductor of the coaxial cable is connected with the metal ground plane of Vivaldi antenna to achieve the conversion of the micro-strip line to the coaxial cable. Adopting the theory of electromagnetic coupling, a micro-strip line is converted to the resonant

https://doi.org/10.1017/S1759078718001113 Published online by Cambridge University Press

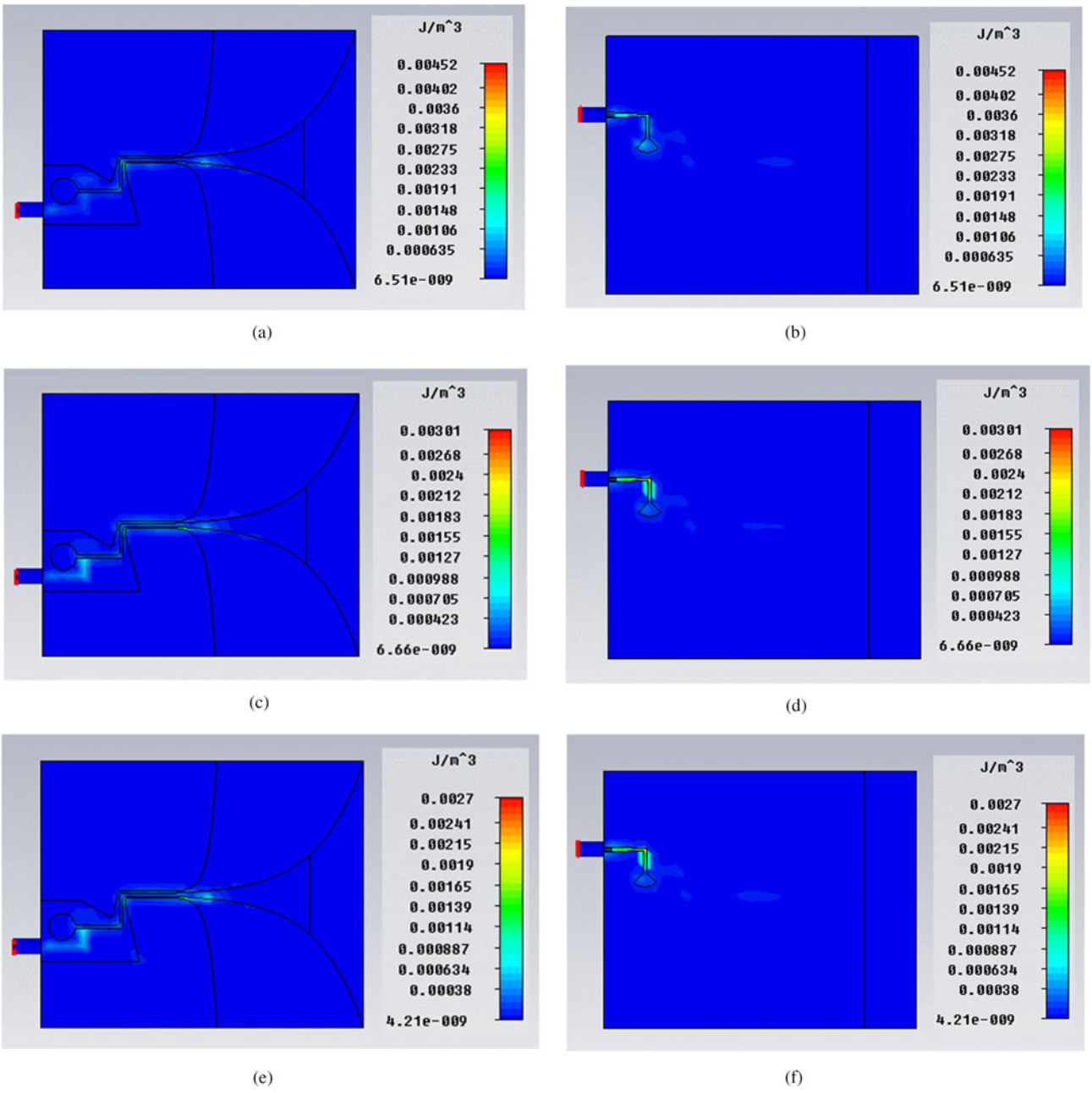

Fig. 5. Simulated electric energy density of port 2, (a) positive structure of electric energy density at 2 GHz, (b) reverse structure of electric energy density at 2 GHz, (c) positive structure of electric, energy density at 2.5 GHz, (d) reverse structure of electric energy density at 2.5 GHz, (e) positive structure of electric energy density at 2.7 GHz, (f) reverse structure of electric energy density at 2.7 GHz.

cavity on the side of the dielectric substrate and slot line. The most prominent advantage of the feed structure is that it avoids the intersection of lines and saves lines.

The exponential printed dipole structure is determined by highest and lowest of working frequency. The exponential tapered curve can be determined by (1) and (2) [17]. $p_1(x_1, y_1)$ and $p_2(x_2, y_2)$ are the beginning and the end points of the exponential tapered curve.

$$y = C_1 e^{\alpha x} + C_2, \tag{1}$$

$$C_1 = \frac{y_2 - y_1}{e^{\alpha x_2} - e^{\alpha x_1}}, C_2 = \frac{y_1 e^{\alpha x_2} - y_2 e^{\alpha x_1}}{e^{\alpha x_2} - e^{\alpha x_1}}. \tag{2}$$

The size of coplanar strip line depends on the calculation formula of micro-strip impedance [18],

$$Z = \frac{87}{\sqrt{\varepsilon_r + 1.41}} \ln\left(\frac{5.98H}{0.8W + T}\right), \tag{3}$$

where H is the thickness of the dielectric substrate, W is the width of the coplanar strip line, and T is the thickness of the coplanar

https://doi.org/10.1017/S1759078718001113 Published online by Cambridge University Press

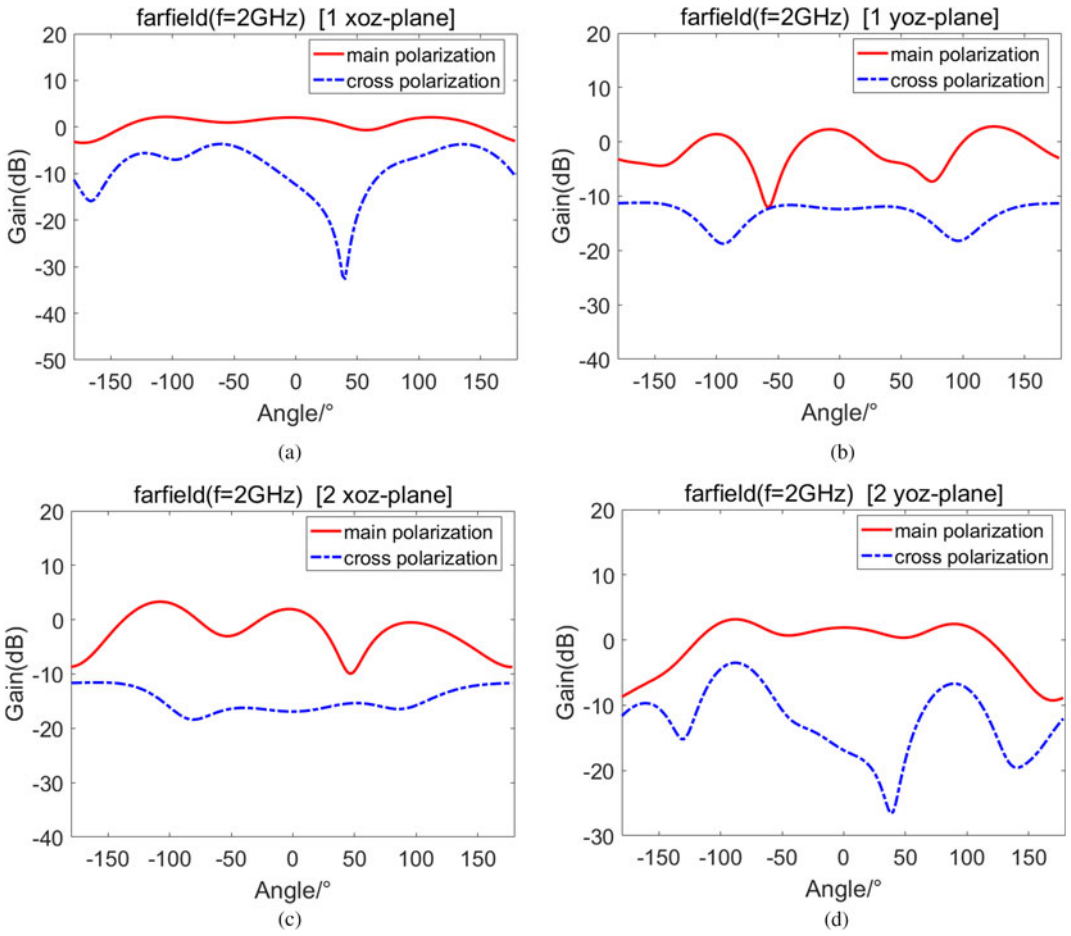

Fig. 6. The radiation pattern at 2 GHz, (a) the pattern of port 1 at *xoz* plane, (b) the pattern of port 1 at *yoz* plane, (c) the pattern of port 2 at *xoz* plane, (d) the pattern of port 2 at *yoz* plane.

strip line. The size of slot line is determined by the calculation formula of slot line impedance [19] when $3.8 \le \varepsilon_r \le 9.8$, $0.0015 \le w\_sl/\lambda_0 \le 0.075$,

$$\begin{aligned} Z_0 = {} & 73.6 - 2.15\varepsilon_r + (638.9 - 31.37\varepsilon_r)\left(w\_sl/\lambda_0\right)^{0.6} \\ & + \left(36.23\sqrt{\varepsilon_r^2 + 41} - 225\right)\frac{w\_sl/H}{\left(w\_sl/H + 0.876\varepsilon_r - 2\right)} \\ & + 0.51(\varepsilon_r + 2.12)\left(w\_sl/H\right)\ln\left(100H/\lambda_0\right) \\ & - 0.753\varepsilon_r\left(H/\lambda_0\right)/\sqrt{w\_sl/\lambda_0}, \end{aligned} \tag{4}$$

where w_sl is the width of the slot line. The calculation formulas help to establish a preliminary antenna model, and the final model is decided by simulated results. The size of coplanar strip line and slot line is determined by impedance, and there is no effective method for slot position, which is determined by simulated results.

In this paper, the optimal structure is shown in Fig. 2 and the optimal size is shown in Table 1. The diameter of the inner conductor is 1.27 mm, and the influence of coaxial cable on the antenna performance is as small as possible. In the curvature of exponential taper, α is 0.06 and 0.35. W is 0.5 mm.

The electromagnetic simulation of the dual-polarized Vivaldi antenna with improved balun feed

In this paper, the electromagnetic simulation software is used to simulate the radiation performance of the presented antenna. According to the performance requirements, the antenna structure of dual-polarized Vivaldi antenna is designed. The return loss of ports 1 and 2 is shown in Figs 3(a) and 3(b). The return loss of ports 1 and 2 is <−10 dB. The isolation between two polarization ports is shown in Fig. 3(c). The VSWR of port 1 and the VSWR of port 2 are both around 1.5 within the frequency range of 2–3.5 GHz. The isolation between two polarization ports is < −15 dB in the operating frequency band.

Figs 4 and 5 show the electric energy density of the proposed antenna at 2, 2.5, and 2.7 GHz. According to the electric energy density, both the energy distribution and the current transmission path are clear.

The antenna radiation direction is along the x-axis. Then the overall structure of the antenna is rotated so that the maximum radiation direction is along the z-axis. The simulation radiation patterns of dual-polarized Vivaldi antenna at 2, 2.5, and 2.7 GHz are presented in Figs 6, 7, and 8, respectively. At each frequency point, the radiation patterns of the two polarization ports at the *xoz* and *yoz* planes are provided, respectively. According to the simulated radiation patterns, it can be observed that the designed antenna has wide radiation, regular pattern shape, and

https://doi.org/10.1017/S1759078718001113 Published online by Cambridge University Press

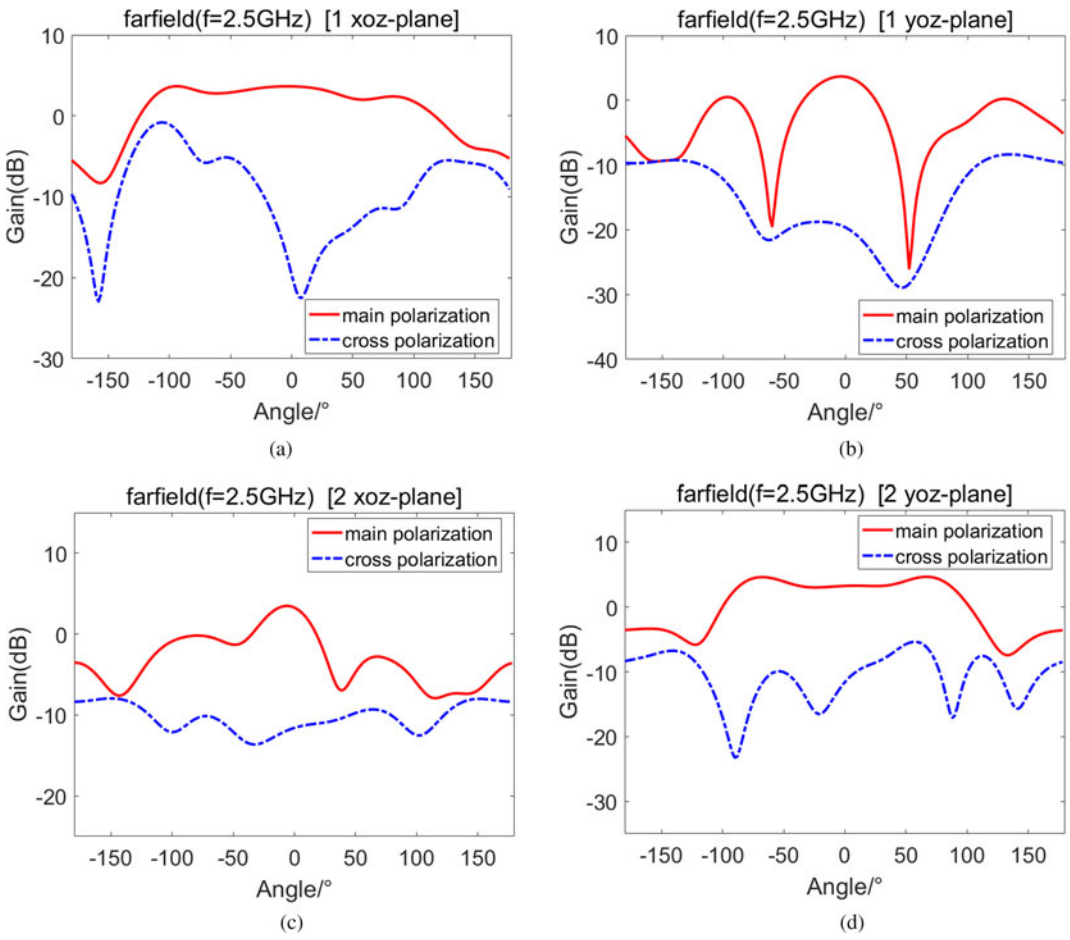

Fig. 7. The radiation pattern at 2.5 GHz, (a) the pattern of port 1 at *xoz* plane, (b) the pattern of port 1 at *xoz* plane, (c) the pattern of port 2 at *xoz* plane, (d) the pattern of port 2 at *yoz* plane.

low back lobe. The beam shape is more regular, and the radiation gain of the two polarized ports is basically equal, and both of them are >2 dB.

The simulation accuracy mainly depends on the discretization of the structure. The accuracy can be improved by the encryption grid, and truncation error in transient simulation is a source of error. The curve of *S* parameter procedures ripples waves due to truncation error. The influence of simulation accuracy on circuit characteristics of the proposed antenna is shown in Fig. 9. According to the comparison diagram of simulated results of *S* parameter, no matter the accuracy is one-thousandth, one ten-thousandth or one hundred-thousandth, the simulated results of S_{11} and S_{21} are basically consistent. When accuracy is one-thousandth, the simulated result of S_{22} is not more precise than other accuracy, but the simulated results is accurate and reliable.

In this section, the influence of several key parameters on the performance of the antenna circuit is discussed such as the diameter of the fan-shaped matching branch, *R_R*. Figure 10 presents the influence of parameter *R_R* on the performance of the antenna circuit. In the range of 2–2.262 GHz, with the increasing of *R_R*, the return loss of port 1 becomes worse, and in the range of 2.62–3.5 GHz, the return loss of port 1 becomes better. In the range of 2–3.5 GHz, with the increasing of *R_R*, the return loss of port 2 becomes better. *R_R* has little effect on the isolation between two polarization ports. Thus, the optimal result of *R_R* is 5 mm.

The influence of parameter *w_st* on the antenna circuit performance is shown in Fig. 11. As the *w_st* varies from 0.5 to 1.5 mm, the resonance frequency moves toward the low-frequency part. *w_st* has little effect on isolation between two polarization ports, too.

Fabrication and test of dual-polarized Vivaldi antenna with improved balun feed

According to the designed antenna structure and size, the dual-polarized Vivaldi antenna has been fabricated and its prototype photo is shown in Fig. 12.

The measured results of input circuit characteristics of fabricated dual-polarized Vivaldi antenna are shown in Fig. 13. The measured results are measured in the microwave dark room meeting design requirements. The measured results have certain differences from the simulation results. The return loss of measured results is basically <−10 dB at the operation frequency range and the polarization port isolation is <−25 dB. The measured result of isolation degree is better than simulated results. The measured result of S_{22} is basically better than the simulated result, especially at high frequencies. The measured result of S_{11} at high frequencies is basically better than the simulated result, but the

https://doi.org/10.1017/S1759078718001113 Published online by Cambridge University Press

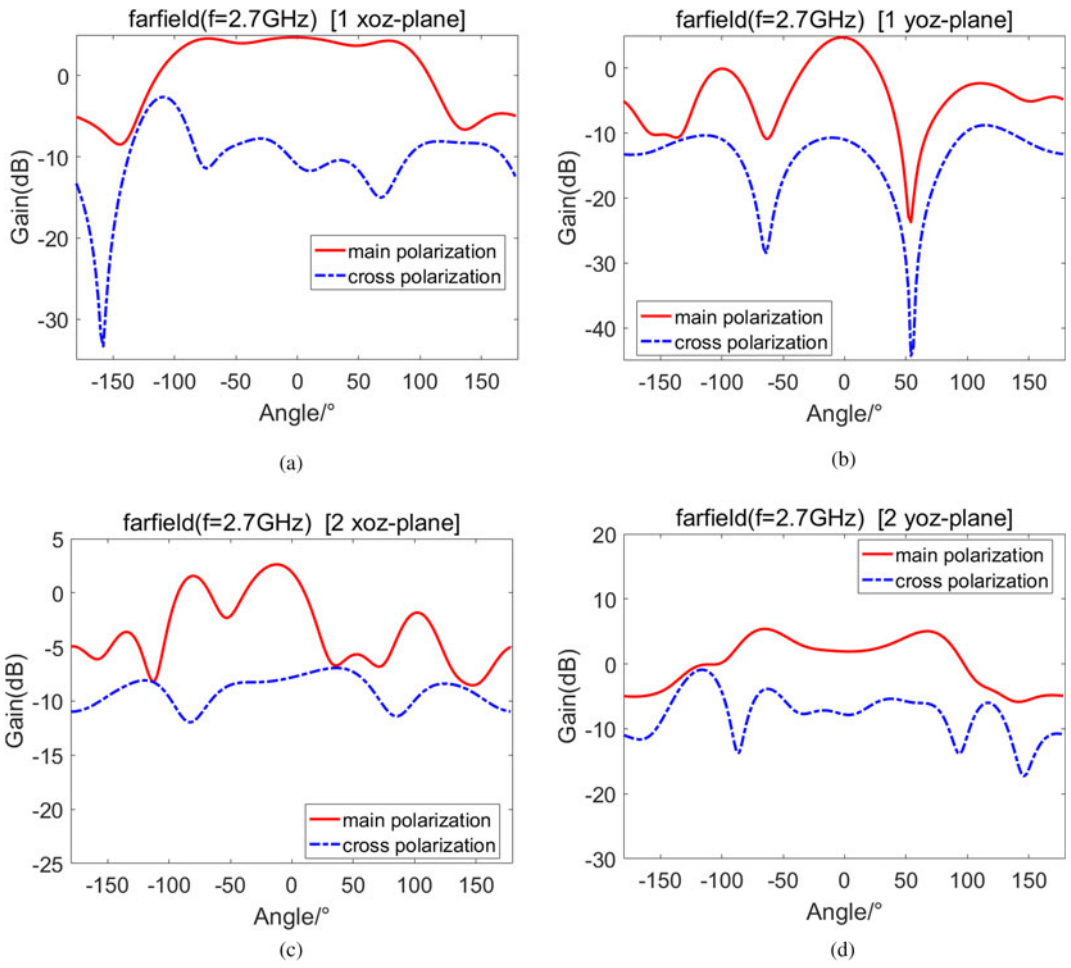

Fig. 8. The radiation pattern at 2.5 GHz, (a) the pattern of port 1 at *xoz* plane, (b) the pattern of port 1 at *yoz* plane, (c) the pattern of port 2 at *xoz* plane, (d) the pattern of port 2 at *yoz* plane.

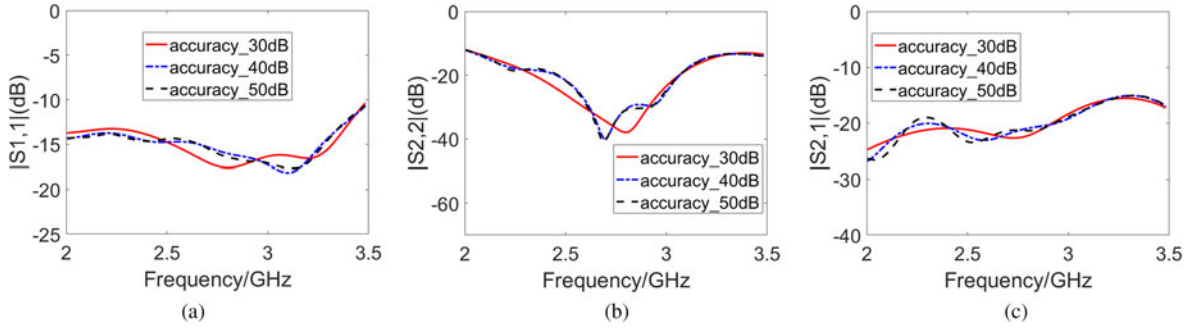

Fig. 9. The influence of simulation accuracy on circuit characteristics proposed antenna, (a) the influence of simulation accuracy on S_{11}, (b) the influence of simulation accuracy on S_{22}, (c) the influence of simulation accuracy on S_{21}.

measured result of S_{11} at low frequencies is worse than the simulated result. Generally, the measured result of return loss and VSWR are better than the simulated results due to the loss of transmission line. That is because material error and processing error cause the difference and the resonance is undesirable.

The measured results of radiation patterns at 2, 2.5, and 2.7 GHz for the dual-polarized Vivaldi antenna are presented in Figs 14, 15, and 16, respectively. In order to compare with the radiation pattern of simulated results, the processed antenna is rotated to make the direction of radiation along *z*-axis. Each graph gives the radiation pattern of two ports at the *xoz* and *yoz* planes, respectively. As shown in the figures, the main polarization of tested results is similar to the simulated results, and the cross-polarization of tested results is basically better than the

https://doi.org/10.1017/S1759078718001113 Published online by Cambridge University Press

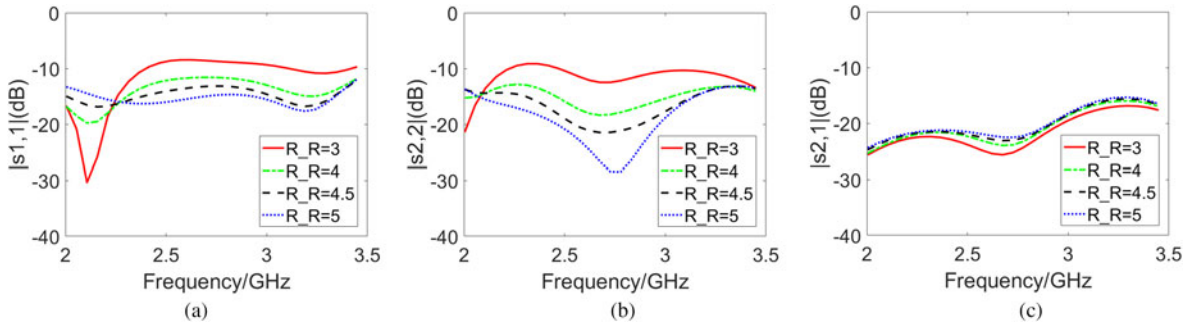

Fig. 10. The influence of parameter *R_R* on circuit characteristics proposed antenna, (a) the influence of *R_R* on return loss of port 1, (b) the influence of *R_R* on return loss of port 2, (c) the influence of *R_R* on isolation.

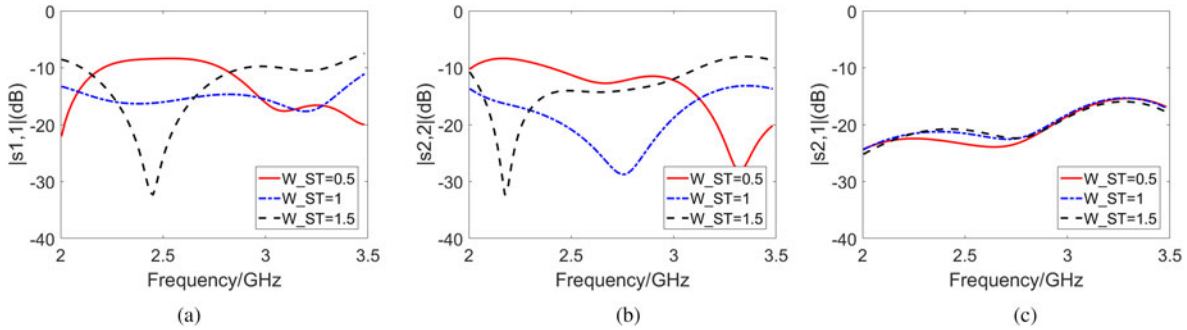

Fig. 11. The influence of parameter *w_st* on circuit characteristics proposed antenna, (a) the influence of *w_st* on return loss of port 1, (b) the influence of *w_st* on return loss of port 2, (c) the influence of *w_st* on isolation.

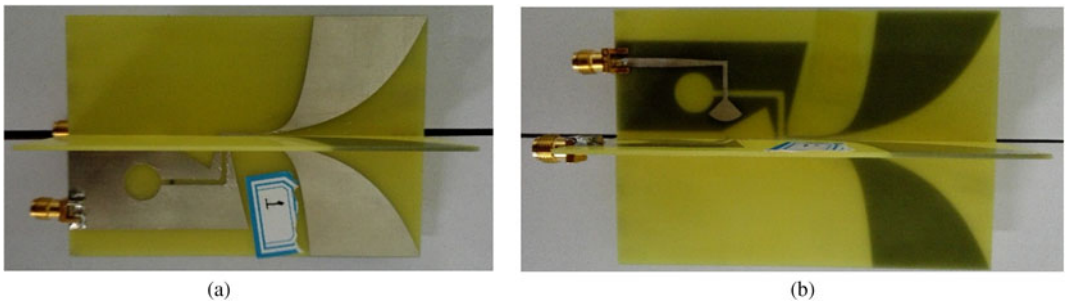

Fig. 12. The prototype photo of dual-polarized Vivaldi antenna with improved balun feed.

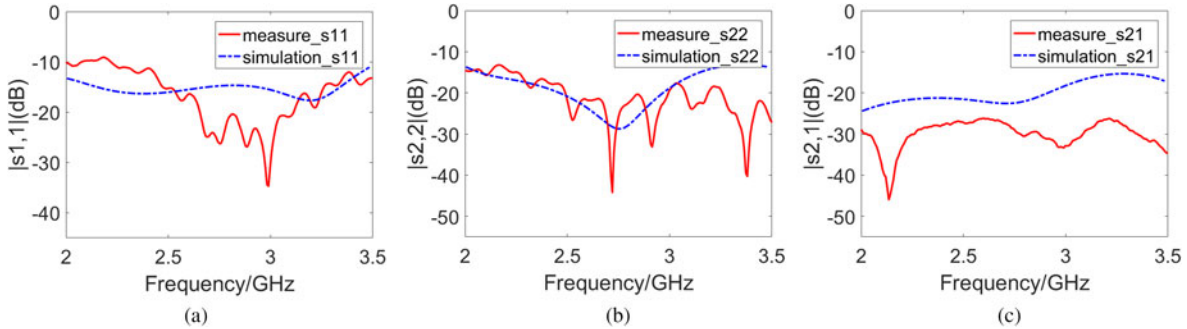

Fig. 13. The circuit characteristics of fabricated dual-polarized Vivaldi antenna, (a) the return loss of port 1, (b) the return loss of port 2, (c) the isolation between two polarization ports.

https://doi.org/10.1017/S1759078718001113 Published online by Cambridge University Press

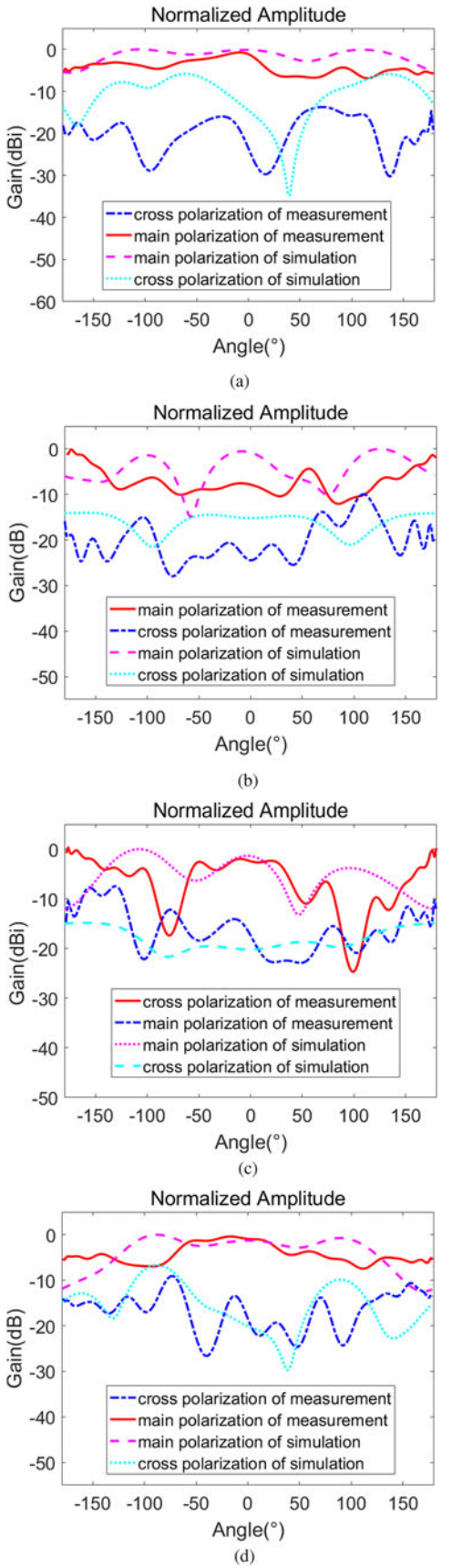

Fig. 14. The radiation pattern at 2 GHz, (a) the pattern of port 1 at *xoz* plane, (b) the pattern of port 1 at *yoz* plane, (c) the pattern of port 2 at *xoz* plane, (d) the pattern of port 2 at *yoz* plane.

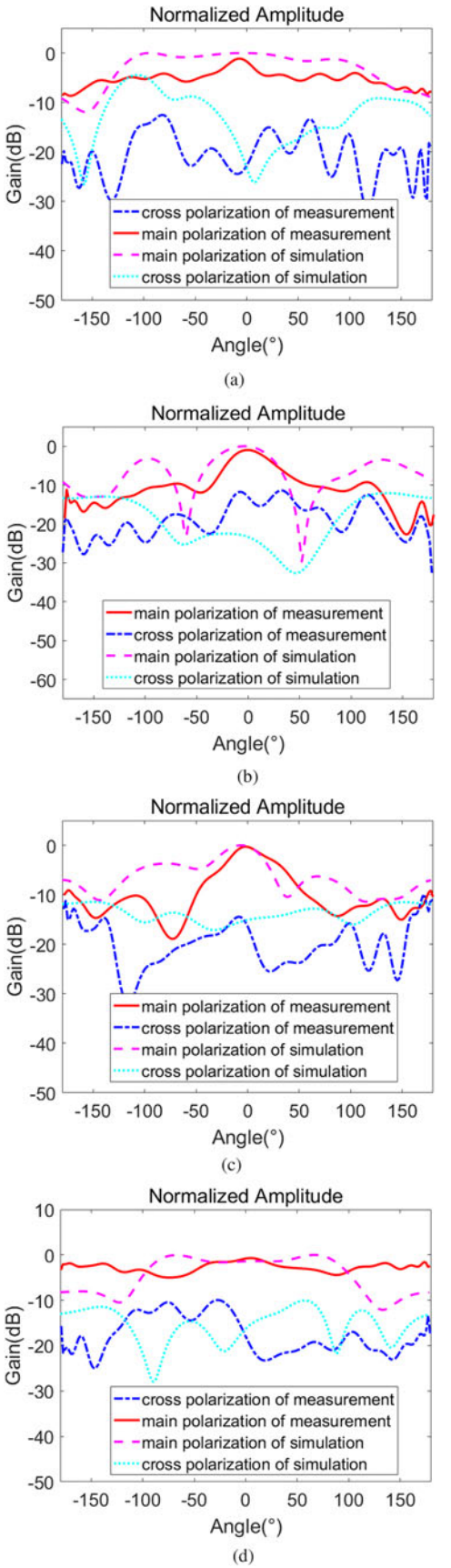

Fig. 15. The radiation pattern at 2.5 GHz, (a) the pattern of port 1 at *xoz* plane, (b) the pattern of port 1 at *yoz* plane, (c) the pattern of port 2 at *xoz* plane, (d) the pattern of port 2 at *yoz* plane.

https://doi.org/10.1017/S1759078718001113 Published online by Cambridge University Press

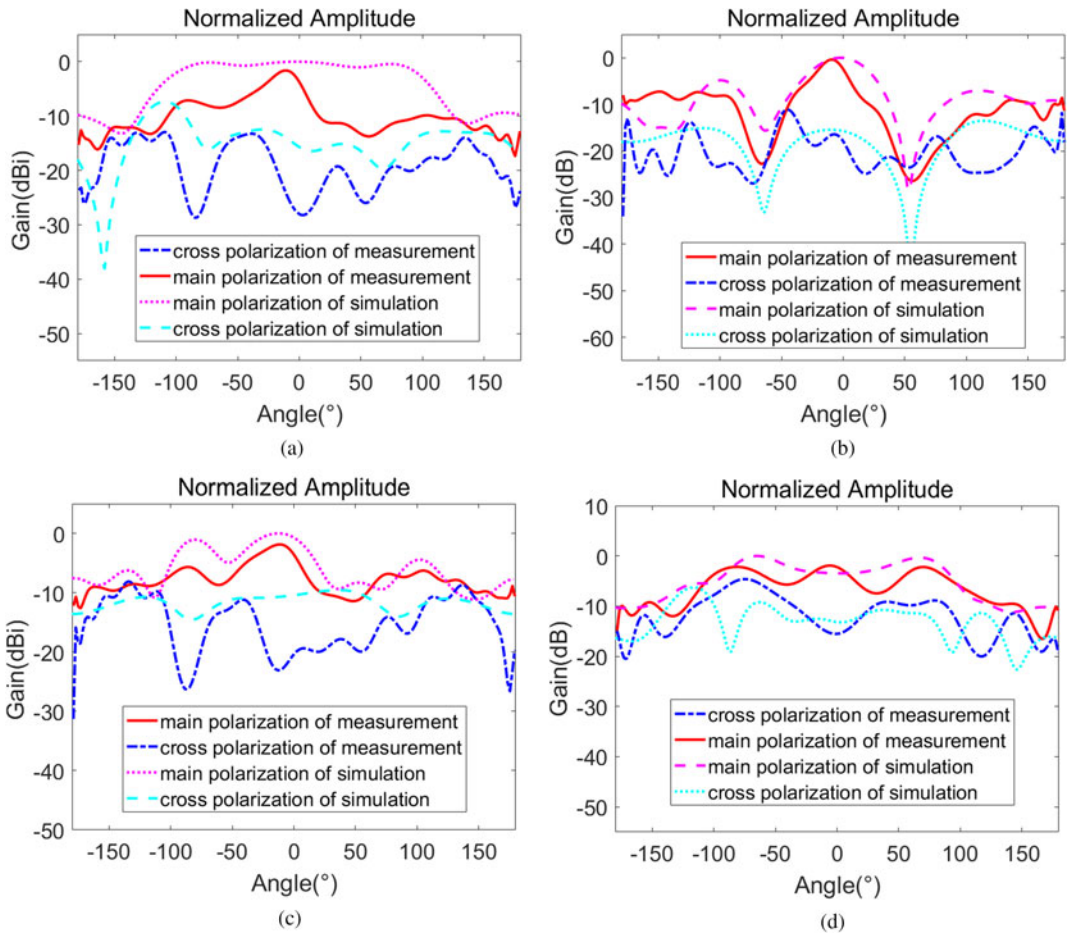

Fig. 16. The radiation pattern at 2.7 GHz, (a) the pattern of port 1 at *xoz* plane, (b) the pattern of port 1 at *yoz* plane, (c) the pattern of port 2 at *xoz* plane, (d) the pattern of port 2 at *yoz* plane.

simulated results. But the beam width of simulated results is larger than the tested results. That is because material error and processing error cause the difference and the resonance is undesirable.

The performance indicators of *xoz* plane of port 1 and the *yoz* plane of port 2 are better than the performance indicators of the *yoz* plane of port 1 and the *xoz* plane of port 2. That is because the antenna is end-fire antenna, whose direction of radiation is parallel to the exponential-printed dipole structure. The beam width of plane that is parallel to the exponential-printed dipole structure is larger than the beam width of plane that is vertical to the structure. Based on the antenna technical indices such as VSWR and radiation patterns, the researched dual-polarized antenna is suitable for some application fields such as passive electronic reconnaissance, passive radar, and wideband communication and detection.

Conclusion

Using polarization information processing technology to develop polarized radar is an effective approach to solve some problems. A dual-polarized antenna can receive all polarization information of electromagnetic waves. Thus, a dual-polarization antenna is a key technology in some fields such as passive radar and wideband communication and detection. In this paper, the wideband dual-polarized Vivaldi antenna with improved balun feed is presented and is composed of two Vivaldi antenna elements, which are orthogonally located. Each Vivaldi antenna element is fed by employing the electromagnetic coupling from micro-strip line to slot line. The most prominent advantage of the feed structure is that it avoids the intersection of lines and saves lines due to bending of the strip line. Performance indices can be applied to practical engineering projects. The research results in this paper can provide a useful technical reference for the practical engineering application.

Acknowledgement. This work is sponsored by the National Natural Science Foundation of China (Grant No. 61571154) and the Science Foundation of Aeronautics of China (Grant No. 20160177005).

References

1. **Yang Z, Jiao Y, Zhou L and Luo X** (2016) A broadband dual-polarized directional antenna with high-gains. *Journal of Microwave* **32**, 478–481.
2. **Yu D, Wu H, He B and Zhu R** (2011) An antenna element for dual-polarized wide-band wide-angle phased array. *Modern Radar* **33**, 59–62.
3. **Ren Y, Ding J and Guo C** (2017) Design of a high-gain wideband dual-polarized antenna based on split ring resonators. *Journal of Electronics & Information Technology* **39**, 2790–2794.
4. **Wang J, Shen Z and Zhao L** (2017) Wideband dual-polarized antenna for spectrum monitoring systems. *IEEE Antennas and Wireless Propagation Letters* **16**, 2236–2239.

https://doi.org/10.1017/S1759078718001113 Published online by Cambridge University Press

5. **Zhu F, Gao S, Ho ATS, Abd-Alhameed RA, See CH, Brown TWC, Li J, Wei G and Xu J** (2014) Ultra-wideband dual-polarized patch antenna with four capacitively coupled feeds. *IEEE Transactions on Antennas and Propagation* **62**, 2440–2449.
6. **Adamiuk G, Zwick T and Wiesbeck W** (2010) Compact, dual-polarized UWB-antenna, embedded in a dielectric. *IEEE Transactions on Antennas and Propagation* **58**, 279–286.
7. **Ding K, Gao C, Wu Y, Qu D, Zhang B and Wang Y** (2017) Dual-band and dual-polarized antenna with end-fire radiation. *IET Microwaves, Antennas & Propagation* **11**, 1823–1828.
8. **Saxena S, Kanaujia BK, Dwari S, Kumar S and Tiwari R** (2017) A compact dual-polarized MIMO antenna with distinct diversity performance for UWB applications. *IEEE Antennas and Wireless Propagation Letters* **16**, 3096–3099.
9. **Sonkki M, Sánchez-Escuderos D, Hovinen V, Salonen ET and Ferrando-Bataller M** (2015) Wideband dual-polarized cross-shaped vivaldi antenna. *IEEE Transactions on Antennas and Propagation* **63**, 2813–2819.
10. **Yan JB, Gogineni S, Camps-Raga B and Brozena J** (2016) A dual-polarized 2–18-GHz vivaldi array for airborne radar measurements of snow. *IEEE Transactions on Antennas and Propagation* **64**, 781–785.
11. **Hung Loui J, Weem P and Popovic Z** (2003) A dual-band dual-polarized nested Vivaldi slot array with multilevel ground plane. *IEEE Transactions on Antennas and Propagation* **51**, 2168–2175.
12. **Yang D, Liu S and Geng D** (2017) A miniaturized ultra-wideband vivaldi antenna with low cross polarization. *IEEE Access* **5**, 23352–23357.
13. **Wu W, Wei G, Zhao W and Li W** (2014) Design of broadband circular polarization Vivaldi antenna array for X-band applications. *Electronic Design Engineering* **22**, 95–98.
14. **Xu T, Zhang H, Wang D, Zhu H and Lan M** (2013) Design of wideband circular polarized Vivaldi array with high gain. *High Power Laser and Particle Beams* **25**, 685–688.
15. **Kang X, Chen L and Li Z** (2017) A modified UWB antipodal vivaldi antenna with improved radiation characteristics. *Journal of Communication University of China (Science and Technology)* **24**, 15–18.
16. **Zhang G, Wang W, Huo X, Yang C and Wang X** (2017) A design of UWB dual-polar Vivaldi antenna. *Space Electronic Technology* **14**, 57–60.
17. **Bian L, Lv Z, Jin B and Sun F** (2008) Research on the design of ultra wideband Vivaldi antenna. *Mobile Communications* 80–83.
18. **Yu W, Li X, Wu B, Wu F and Qian Y** (2015) Analysis of compensation of micro-strip line impedance discontinuity. *Instrument Technique and Sensor* 88–91.
19. **Janaswamy R and Schaubert DH** (1986) Characteristic impedance of a wide slot line on low-permittivity substrates (short paper). *IEEE Transactions on Microwave Theory and Techniques* **8**, 900–902.

Lizhong Song was born in 1975. He received the Master degree and Ph.D. degree from Harbin Institute of Technology in 2001 and 2005, respectively. He is a professor and doctoral supervisor of Harbin Institute of Technology at Weihai. He focuses his academic interests on antenna design, wireless electromagnetic wave propagation, microwave technology, and radar signal processing.

Huiyuan Zhou received the B.E. degree in Electrical Engineering and Automation from Xi'an Jiaotong University City College, China, in 2016. Currently, she is a master student in the School of Information and Electrical Engineering at Harbin Institute of Technology, China. Her research interests include dual-polarized conformal array antenna and direction of arriving estimation theory and methods.

https://doi.org/10.1017/S1759078718001113 Published online by Cambridge University Press